From the Characterization of the Four Serine/Threonine Protein Kinases (PknA/B/G/L) of Corynebacterium glutamicum toward the Role of PknA and PknB in Cell Division.

Maria Fiuza, Marc J Canova, Isabelle Zanella-Cléon, Michel Becchi, Alain J Cozzone, Luís M Mateos, Laurent Kremer, José A Gil, Virginie Molle

THE JOURNAL OF BIOLOGICAL CHEMISTRY VOL. 283, NO. 26, pp. 18099–18112, June 27, 2008

From the Characterization of the Four Serine/Threonine Protein Kinases (PknA/B/G/L) of *Corynebacterium glutamicum* toward the Role of PknA and PknB in Cell Division*

Received for publication, April 3, 2008, and in revised form, April 24, 2008 Published, JBC Papers in Press, April 28, 2008, DOI 10.1074/jbc.M802615200

Maria Fiuza[‡1], Marc J. Canova[§], Isabelle Zanella-Cléon[§], Michel Becchi[§], Alain J. Cozzone[§], Luís M. Mateos[‡], Laurent Kremer[¶‖], José A. Gil[‡], and Virginie Molle[§2]

From the [‡]Departamento de Biología Molecular, Área de Microbiología, Facultad de Biología, Universidad de León, León 24071, Spain, the [§]Institut de Biologie et Chimie des Protéines, UMR 5086, CNRS, Université Lyon 1, IFR128 BioSciences, Lyon-Gerland, 7 Passage du Vercors, 69367 Lyon Cedex 07, France, the [¶]Laboratoire de Dynamique des Interactions Membranaires Normales et Pathologiques, Université de Montpellier II et I, CNRS, UMR 5235, Case 107, Place Eugène Bataillon, 34095 Montpellier Cedex 05, France, and [‖]INSERM, DIMNP, Place Eugène Bataillon, 34095 Montpellier Cedex 05, France

Corynebacterium glutamicum **contains four serine/threonine protein kinases (STPKs) named PknA, PknB, PknG, and PknL. Here we present the first biochemical and comparative analysis of all four *C. glutamicum* STPKs and investigate their potential role in cell shape control and peptidoglycan synthesis during cell division. *In vitro* assays demonstrated that, except for PknG, all STPKs exhibited autokinase activity. We provide evidence that activation of PknG is part of a phosphorylation cascade mechanism that relies on PknA activity. Following phosphorylation by PknA, PknG could transphosphorylate its specific substrate OdhI *in vitro*. A mass spectrometry profiling approach was also used to identify the phosphoresidues in all four STPKs. The results indicate that the nature, number, and localization of the phosphoacceptors varies from one kinase to the other. Disruption of either *pknL* or *pknG* in *C. glutamicum* resulted in viable mutants presenting a typical cell morphology and growth rate. In contrast, we failed to obtain null mutants of *pknA* or *pknB*, supporting the notion that these genes are essential. Conditional mutants of *pknA* or *pknB* were therefore created, leading to partial depletion of PknA or PknB. This resulted in elongated cells, indicative of a cell division defect. Moreover, overexpression of PknA or PknB in *C. glutamicum* resulted in a lack of apical growth and therefore a coccoid-like morphology. These findings indicate that *pknA* and *pknB* are key players in signal transduction pathways for the regulation of the cell shape and both are essential for sustaining corynebacterial growth.**

Corynebacterium glutamicum is a leading industrial amino acid producer and a model organism of the Corynebacteriaceae, a suborder of the actinomycetes that also includes the genus *Mycobacterium*. This soil-borne, nonpathogenic Gram-positive actinomycete, which is widely used in the industrial production of amino acids, such as L-lysine and L-glutamic acid (1), has been extensively studied leading to the development of efficient genetic manipulation systems (3).

The genetics of cell growth and cell division of *C. glutamicum* started even before the complete genome sequence was available. The earliest studies focused on the sequencing and characterization of corynebacterial genes present in the conserved division and cell wall cluster (2). Once the genome sequence was available, it was evident that this bacterium, as well as different members of the actinomycetes, was deficient in many essential genes for cell division (3) and therefore corresponded to a minimalist version of a more sophisticated cell division apparatus (divisome) present in other bacteria. For instance, *C. glutamicum* is lacking genes homologue to *ftsA* (an actin homologue), to positive regulators involved in FtsZ polymerization such as *zipA* or *zapA*, or to negative regulators such as *ezrA*, *noc*, *slmA*, *sulA*, and *minCD* (3). Moreover, several essential cell division genes (*i.e. ftsN* and *ftsL*) are absent in *C. glutamicum*. Unlike other bacterial models, peptidoglycan (PG)[3] biosynthesis in corynebacteria occurs at the septum and the cell poles (4, 5) and not at the lateral cell wall like in *Bacillus subtilis* or *Escherichia coli.* With respect to PG biosynthesis, *C. glutamicum* possesses only nine penicillin-binding proteins, in contrast to *E. coli* or *B. subtilis* that contain 13 and 16 penicillin-binding proteins, respectively (6). The mechanism by which *C. glutamicum* shifts between synthesis of PG at mid-cell for cell division or at the cell poles for cell elongation remains unclear, although this process is likely to be regulated in response to different stimuli encountered during growth.

Protein phosphorylation is a key mechanism by which environmental signals are transmitted to control protein activities in both eukaryotic and prokaryotic cells. Three main superfamilies of protein kinases are described as follows, the first one includes the "eukaryotic like" serine/threonine protein kinases

* This work was supported in part by grants from the Region Rhone-Alpes (to M. C.), the CNRS, the University of Lyon (France), National Research Agency Grant ANR-06-MIME-027-01 (to V. M. and L. K.), Junta de Castilla y León Grant LE040A07 (to J. A. G.), and Ministerio de Ciencia y Tecnología (Spain) Grants BIO2008-03234 and BIO2005-02723 (to J. A. G. and L. M. M.). The costs of publication of this article were defrayed in part by the payment of page charges. This article must therefore be hereby marked "*advertisement*" in accordance with 18 U.S.C. Section 1734 solely to indicate this fact.

[1] Recipient of a fellowship from the Ministerio de Educación y Ciencia.

[2] To whom correspondence should be addressed. Tel.: 33-4-72-72-26-79; Fax: 33-4-72-72-26-41; E-mail: vmolle@ibcp.fr.

[3] The abbreviations used are: PG, peptidoglycan; STPK, serine/threonine protein kinase; GST, glutathione *S*-transferase; MS/MS, tandem mass spectrometry; DAPI, 4′,6-diamino-2-phenylindole; PASTA, penicillin-binding protein and serine/threonine kinase-associated; Ni-NTA, nickel-nitrilotriacetic acid; TEV, tobacco etch virus; Van-FL, fluorescent vancomycin.

TABLE 1

Bacterial strains and plasmids used in this study

The abbreviation used is as follows: nt, nucleotide.

Strains or plasmids	Genotype or description	Source or Ref.
E. coli TOP10	F$^-$ *mcr*A Δ(*mrr-hsd*RMS-*mcr*BC) φ80*lacZ*Δ*M15* Δ*lacX74 deoR recA1 araD139* Δ(*ara-leu*)7697 *galU galK rpsL endA1 nupG*; used for general cloning	Invitrogen
E. coli S17-1	Mobilizing donor strain, *pro recA*, which possesses an RP4 derivative integrated into the chromosome	62
E. coli BL21(DE3)Star	F2 *ompT hsdSB*(rB2 mB2) *gal dcm* (DE3); used to express recombinant proteins in *E. coli*	Stratagene
C. glutamicum ATCC 13869	Wild type control strain	ATCC
C. glutamicum R31	*C. glutamicum* ATCC 13869; derivative used as recipient in conjugations	63
pGEM-TEasy	*E. coli* vector; *bla lacI orif1*	Promega
pK18mob	Mobilizable plasmid containing a *E. coli* origin of replication and *kan* resistance gene	64
pKAint	pK18mob derivative carrying an internal 485-bp fragment of *pknA* from *C. glutamicum*	This work
pKBint	pK18mob derivative carrying an internal 502-bp fragment of *pknB* from *C. glutamicum*	This work
pKGint	pK18mob derivative carrying an internal 849-bp fragment of *pknG* from *C. glutamicum*	This work
pKLint	pK18mob derivative carrying an internal 754-bp fragment of *pknL* from *C. glutamicum*	This work
pKLA	pK18mob derivative carrying the 5′-end (472 nt) of *pknA* from *C. glutamicum* under control of the P_{lac} promoter	This work
pKLB	pK18mob derivative carrying the 5′-end (470 nt) of *pknB* from *C. glutamicum* under control of the P_{lac} promoter	This work
pKPD	pK18mob derivative carrying the 5′-end (550 nt) of *divIVA* under the control of the *C. glutamicum gntK* gene promoter (P_{gntK}-Δ*divIVA*$_{CG}$)	2
pKPKA	pKPD derivative carrying the 5′-end (472 nt) of *pknA* under the control of the *C. glutamicum gntK* gene promoter (P_{gntK}-Δ*pknA*$_{CG}$)	This work
pKPKB	pKPD derivative carrying the 5′-end (470 nt) of *pknB* under the control of the *C. glutamicum gntK* gene promoter (P_{gntK}-Δ*pknB*$_{CG}$)	This work
pECM2	Mobilizable plasmid able to replicate in *E. coli* and *C. glutamicum*; *kan* and *cat* resistance genes	65
pEDiv	pECM2 derivative carrying P*div*	A. Ramos, unpublished data
pECDA	pEDiv derivative carrying P*div-pknA*	This work
pECDB	pEDiv derivative carrying P*div-pknB*	This work
pECDG	pEDiv derivative carrying P*div-pknG*	This work
pECDL	pEDiv derivative carrying P*div-pknL*	This work
pGEX4T-3	*E. coli* vector designed to make GST gene fusions	GE Healthcare
pGEXA	pGEX4T-3 derivative used to express GST fusion of PknA cytoplasmic domain	This work
pGEXB	pGEX4T-3 derivative used to express GST fusion of PknB cytoplasmic domain	This work
pGEXL	pGEX4T-3 derivative used to express GST fusion of PknL cytoplasmic domain	This work
pETTev	pET15b (Novagen) derivative that includes the replacement of the thrombin site coding sequence with a TEV protease site	21
pTEVGfull	pETTev derivative used to express His-tagged PknG	This work
pTEVOdhI	pETTev derivative used to express His-tagged OdhI	This work

(STPKs) (7–9); the second one corresponds to the newly characterized prokaryotic class of tyrosine kinases (10); and the third one corresponds to the well known family of bacterial kinases, the sensor histidine kinases, which are key enzymes of the so-called "two-component systems" (11). In bacteria, the presence of several STPKs suggests a central role of protein phosphorylation in regulating various biological functions, ranging from environmental adaptive responses to bacterial pathogenicity, like in the actinomycete relative *Mycobacterium tuberculosis* (12, 13). Thus, regulatory devices involving STPKs and phosphatases represent an emerging theme in prokaryotic signaling cascades. We therefore addressed the question whether STPKs could be involved in the model of growth in *C. glutamicum*.

In silico analysis of the genome sequence of *C. glutamicum* predicted the presence of four different STPKs (14). Three of these appear to be transmembrane proteins, with a putative extracellular signal sensor domain and an intracellular kinase domain. One of them, PknG, presented as a soluble kinase, has been investigated for its physiological role (15). Recent studies have demonstrated that in *M. tuberculosis* the STPKs PknA and PknB regulate cell growth (16) and cell division (17, 18). Because of the conserved genetic organization of the *pknA*/*pknB* cluster in *M. tuberculosis* and *C. glutamicum*, it is tempting to speculate that cell shape and division are also regulated by phosphorylation in *C. glutamicum.*

In this study, we focused on the four putative STPKs of *C. glutamicum*. As a first step in deciphering the potential role/participation of these kinases in the cell division process, the four proteins were characterized biochemically through a combination of *in vitro* phosphorylation assays and mass spectrometric analysis of their phosphorylation sites. We also demonstrated that either overexpression or depletion of PknA and PknB in *C. glutamicum* causes major growth and morphological changes, very likely resulting from cell division and cell wall biosynthesis alterations.

EXPERIMENTAL PROCEDURES

Bacterial Strains, Growth Conditions, and Conjugal Plasmids—Bacterial strains and plasmids are described in Table 1. Strains used for cloning and expression of recombinant proteins were *E. coli* TOP10 (Invitrogen) and *E. coli* BL21(DE3)Star (Stratagene), respectively. *E. coli* cells were grown and maintained at 37 °C in LB medium supplemented with 100 μg/ml ampicillin and/or 50 μg/ml kanamycin, when required. *C. glutamicum* cells were grown at 30 °C in TSB (trypticase soy broth, Oxoid) or TSA (TSB containing 2% agar) medium supplemented with 12.5 μg/ml kanamycin. Plasmids to be transferred by conjugation from *E. coli* to *C. glutamicum* were introduced by transformation into the donor strain *E. coli* S17-1. Mobilization of plasmids from *E. coli* to coryneform strains was accomplished as described previously (19).

TABLE 2
Primers used in this study

Primer	Gene	5′ to 3′ sequence[a]
pknAint1	*pknA*	GCTCTAGAGCGCGAAGGCAGACTG (XbaI)
pknAint2	*pknA*	TATGGATCCTTGCGCAACGA (BamHI)
pknBint1	*pknB*	CCGGAATTCAACGATTCCACCTCCGCC (EcoRI)
pknBint2	*pknB*	TATGGATCCAAGAAGACCCTGACC (BamHI)
pknGint1	*pknG*	CCGGAATTCCCTCCCTGAAAGAC (EcoRI)
pknGint2	*pknG*	TCCTAAGCTTCTTCGGTGGTAAAG (HindIII)
pknLint1	*pknL*	CCGGAATTCGATTCTGGAGAGTTTTTG (EcoRI)
pknLint2	*pknL*	TCCTAAGCTTCATCGTCAGAATATTCACC (HindIII)
pknAlac1	*pknA*	CCGGAATTCATGAGTCAAGAAGACATCACTG (EcoRI)
pknAlac2	*pknA*	GCAAGCTTGTGATCAGCATGTTGCCCG (HindIII)
pknBlac1	*pknB*	CCGGAATTCGTGACCTTCGTGATCGCT (EcoRI)
pknBlac2	*pknB*	GCTCTAGAGCCGAAGTCCATGACTTTCAC (XbaI)
pknA1	*pknA*	GGAATTCCATATGAGTCAAGAAGACATCAC (NdeI)
pknAK	*pknA*	CTTTTTTTTTAAAGTGATCAGCATGTTGCCCG (DraI)
pknB1	*pknB*	GGAATTCCATATGACCTTCGTGATCGCT (NdeI)
pknBK	*pknB*	TGATATCGCCGAAGTCCATGACTTTCAC (EcoRV)
pknA2	*pknA*	GGAATTCCATATGTCACTGCGCTCCTCCTA CATC (NdeI)
pknB2	*pknB*	GGAATTCCATATGCTATTGCACGAGTGCAGCGA (NdeI)
pknG1	*pknG*	GGAATTCCATATGAAGGATAATGAAGATTTC (NdeI)
pknG2	*pknG*	GGAATTCCATATGCTAGAACCAACTCAG (NdeI)
pknL1	*pknL*	GGAATTCCATATGGCAAACTTGAAGGTCG (NdeI)
pknL2	*pknL*	GGAATTCCATATGCTAAAACGCCCTTACTG (NdeI)
pknAcd1	*pknA*	CCGGAATTCTATGAGTCAAGAAGACATCAC (EcoRI)
pknAcd2	*pknA*	TATATTCTCGAGTCACAATGCCGGAACC (XhoI)
pknBcd1	*pknB*	TATGGATCCACCTTCGTGATCGCTGATCGC (BamHI)
pknBcd2	*pknB*	TATAAGCTTCTAGGCCACTTGGGTGGAGGTGCG (HindIII)
pknLcd1	*pknL*	CGGGATCCATGGCAAACTTGAAGGTC (BamHI)
pknLcd2	*pknL*	TATATTCTCGAGCTAAATTGACCACAACGTCAG (XhoI)
pknGfull2	*pknG*	TAATAGCTGCTAGCCTAGAACCAACTCAGTGGCCG (NheI)
534	*odhI*	TAATAGCTCATATGAGCGACAACAACGGCACCCCG (NdeI)
535	*odhI*	TAATAGCTGCTAGCTTACTCAGCAGGGCCTGCGAGGAAAAC (NheI)
M13–26		CAGGAAACAGCTATGAC

[a] Restriction sites are underlined and indicated in parentheses.

Cloning, Expression, and Purification of PknA, PknB, PknL, and PknG—PCR fragments encoding the cytoplasmic domain corresponding to the kinase domain and the juxtamembrane linker of PknA (residues 1–332 out of 469), PknB (residues 1–313 out of 646), and PknL (residues 1–396 out of 740) were amplified by using *C. glutamicum* ATCC 13869 genomic DNA as a template. The different *pkn* gene fragments coding for the N-terminal cytoplasmic region, with appropriate sites at both ends, were synthesized by PCR amplification using the primer pairs pknAcd1/pknAcd2, pknBcd1/pknBcd2, and pknLcd1/pknLcd2, respectively (Table 2). These DNA fragments were digested with the corresponding restriction enzymes and ligated into vector pGEX4T-3 (see Table 1), digested with the same enzymes, to yield pGEXA, pGEXB, and pGEXL, respectively.

E. coli BL21(DE3)Star cells were transformed with the pGEX4T-3 vector derivatives expressing the $PknA_{CD}$, $PknB_{CD}$, and $PknL_{CD}$ proteins. Recombinant *E. coli* strains harboring the pGEX4T-3 derivatives were used to inoculate 200 ml of LB medium supplemented with ampicillin and incubated at 37 °C with shaking until A_{600} reached 0.5. Isopropyl 1-thio-β-D-galactopyranoside was then added at a final concentration of 0.5 mM, and growth was continued for an additional 3-h period at 30 °C. Recombinant GST kinase cytoplasmic regions were purified on glutathione-Sepharose 4B matrix as described previously (20).

For the cloning, expression, and purification of the cytoplasmic PknG recombinant protein (822 residues), the full-length *pknG* gene was amplified by PCR using *C. glutamicum* ATCC 13869 genomic DNA as a template and the primer pair pknG1 and pknGfull2 (Table 2). This PCR product was digested with the restriction enzymes corresponding to the appropriate sites at both ends and ligated into pETTev (Table 1), the variant of pET15b (Novagen) that includes the replacement of the thrombin site coding sequence with a tobacco etch virus (TEV) protease site (21), yielding pTEVGfull. *E. coli* BL21(DE3)Star cells transformed with this construction were used for expression and purification of His-tagged PknG as described previously (22).

Construction and Purification of OdhI Recombinant Protein—The *odhI* gene was amplified by PCR using *C. glutamicum* ATCC 13869 genomic DNA as a template and the primer pair 534/535, containing an NdeI and NheI restriction site, respectively. This 432-bp amplified product was digested by NdeI and NheI, and ligated into pETTev (Table 1) generating the pTEVOdhI. *E. coli* BL21(DE3)Star cells transformed with this construct were used for expression and purification of His-tagged OdhI as described previously (22). Finally, the purified His-tagged OdhI was treated with TEV protease according to the manufacturer's instructions (Invitrogen).

Gene Inactivation in C. glutamicum—Internal fragments of the *pknA, pknB, pknG,* and *pknL* genes were amplified from the *C. glutamicum* ATCC 13869 chromosome using pknAint1/pknAint2, pknBint1/pknBint2, pknGint1/pknGint2, and pknLint1/pknLint2 primer pairs (Table 2), respectively. The amplified 485-, 502-, 849-, and 754-bp DNA fragments were purified and cloned into pGEM-TEasy (Table 1) and later were digested and subcloned into the conjugative suicide plasmid pK18mob (Table 1), yielding to plasmids pKAint, pKBint, pKGint, and pKLint, respectively (Table 1). All these plasmids were used to disrupt the *C. glutamicum pkn* genes by single recombination. The corresponding DNA inserts were used as probes in South-

ern blot experiments to confirm gene disruption. Total DNA from corynebacteria was isolated using the Kirby method described for *Streptomyces* (23), except that the cells were treated with lysozyme for 4 h at 30 °C. For Southern blot analysis, genomic DNA from different *C. glutamicum* transconjugants were digested with different restriction enzymes and loaded on agarose gels. Samples were transferred to nylon membranes and hybridized with digoxigenin-labeled probes according to the manufacturer's instructions (Roche Applied Science) and conventional protocols. To reduce the PknA or PknB levels in *C. glutamicum*, two sets of plasmids were designed to express either *pknA* or *pknB* under the control of P_{lac} and P_{gntK} promoters. Plasmids pKLA and pKLB were constructed as follows. The first 472-bp *pknA* fragment or the 470-bp *pknB* fragment was amplified by PCR using pknAlac1/pknAlac2 and pknBlac1/pknBlac2, respectively (Table 2), digested with EcoRI and HindIII/XbaI, and subcloned into the EcoRI-HindIII/XbaI sites of pK18mob (Table 1). To place *pknA* or *pknB* under the control of the regulated promoter P_{gntK} (promoter of the *gntK* gene encoding the gluconate kinase from *C. glutamicum*) (2), the 5′-ends of *pknA* (472 bp) and *pknB* (470 bp) were PCR-amplified using the pknA1/pknAK and pknB1/pknAK primer pairs, respectively (Table 2), digested with NdeI and DraI/EcoRV, and subcloned into NdeI/EcoRI (Klenow-filled) digested plasmid pKPD (Table 1), yielding to plasmids pKPKA and pKPKB, respectively. To study the expression of the four *pkn* genes in *C. glutamicum* under the control of the strong promoter P_{div} (promoter of the *divIVA* gene from *C. glutamicum*) (5, 24), plasmids pECDA/B/G/L were constructed as follows: *pknA/B/G/L* were PCR-amplified using the primer pairs pknA1/pknA2, pknB1/pknB2, pknG1/pknG2, or pknL1/pknG2, digested with NdeI, and subsequently cloned under the control of the P_{div} promoter into plasmid pEDiv (Table 1).

Microscopic Techniques—Living *C. glutamicum* cells or cells stained with fluorescent dyes were observed in a Nikon E400 phase contrast and fluorescence microscope. Pictures were taken with a DN100 Nikon digital camera. Vancomycin BODIPY-FL (VAN-FL) (Molecular Probes) staining was performed by adding an equal proportion of unlabeled vancomycin and Van-FL to growing cultures at a final concentration of 1 μg/ml (4). After incubation for 5 min to allow absorption of the antibiotic, cells were directly observed by fluorescence microscopy. Staining with 4′,6-diamino-2-phenylindole (DAPI) was performed as described previously (25).

In Vitro Kinase Assays—*In vitro* phosphorylation of each recombinant kinase (0.5 μg) was carried out for 30 min at 37 °C in a reaction mixture (20 μl) containing buffer P (25 mM Tris-HCl, pH 7.0, 1 mM dithiothreitol, 5 mM $MgCl_2$, 1 mM EDTA) with 200 μCi/ml [γ-^{33}P]ATP corresponding to 65 nM (3000 Ci/mmol) (PerkinElmer Life Sciences). After electrophoresis, gels were soaked in 20% trichloroacetic acid for 10 min at 90 °C, stained with Coomassie Blue, and dried. Radioactive proteins were visualized by autoradiography using direct exposure films. For mass spectrometry analysis, kinases were phosphorylated as described above, excepted that [γ-^{33}P]ATP was replaced with 5 mM ATP.

Sample Preparation and Mass Spectrometry Analysis—Purified GST-$PknA_{CD}$, GST-$PknB_{CD}$, GST-$PknL_{CD}$, and His-PknG were subjected to *in vitro* phosphorylation with nonradioactive ATP prior to resolving on SDS-PAGE. In-gel digestion was performed as described by Shevchenko *et al.* (26) with minor modifications. Samples were reduced with 60 μl of 10 mM dithiothreitol in 50 mM NH_4HCO_3 for 40 min at 56 °C. Alkylation was performed with 60 μl of 55 mM iodoacetamide in 50 mM NH_4HCO_3 for 30 min at room temperature in the dark. The gel pieces were successively dried, re-hydrated, and re-dried using 300 μl of CH_3CN, 200 μl of 50 mM NH_4HCO_3, and 300 μl of CH_3CN, respectively. For proteolytic digestion, the protein-containing gel pieces were treated with 30–40 μl of trypsin (sequence grade, Promega, Madison, WI) for 45 min at 50 °C. A second extraction step was performed using 30 μl of H_2O/CH_3CN/HCOOH (60:36:4; v/v/v) mixture for 30 min at 30 °C, and finally all extracts were pooled and dried in a vacuum concentrator and resuspended in 0.1% trifluoroacetic acid (20 μl).

NanoLC/nanospray/tandem mass spectrometry experiments were performed on a Q-STAR XL instrument (QqTOF) (Applied Biosystems, Courtaboeuf, France) equipped with a nanospray source using a distal coated silica-tip emitter (FS 150-20-10-D-20, New Objective) set at 2300 V. By means of information-dependent acquisition mode, peptide ions within a m/z 400–2000 survey scan mass range were analyzed for subsequent fragmentation (three precursors). Double to quadruple charged ions exceeding a threshold of 10 counts were selected for MS/MS analyses. MS/MS spectra were acquired in the m/z 50–2000 range with a 30-s dynamic exclusion time. The collision energy was automatically set by the software (Analyst 1.1) and was related to the charge of the precursor ion. The MS and MS/MS data were recalibrated using internal reference ions from a trypsin autolysis peptide at m/z 842.510 $[M + H]^+$ and m/z 421.759 $[M + 2H]^{2+}$. Screening for phosphorylated peptides was achieved by the paragon method from the ProteinPilot® data base-searching software (version 2.0, Applied Biosystems). The LC part of the analytical system consisted of an LC-Packings nano-LC (Dionex, Voisins Le Bretonneux, France). Chromatographic separation of peptides was obtained in a C_{18} PepMap micro-precolumn (5 μm; 100 Å; 300 μm × 5 mm; Dionex) and a C_{18} PepMap nano-column (3 μm; 100 Å; 75 μm × 150 mm; Dionex). After injection (1-μl injection volume, pick-up mode, in a 20-μl injection loop), samples were adsorbed and desalted on the pre-column with a H_2O/CH_3CN/trifluoroacetic acid (98:2:0.05; v/v/v) solvent mixture for 3 min at 25 μl/min flow rate. The peptide separation was developed using a linear 60-min gradient from 0 to 60% B, where solvent A was 0.1% HCOOH in H_2O/CH_3CN (95/5) and solvent B was 0.1% HCOOH in H_2O/CH_3CN (20/80) at ~200 nl/min flow rate.

RESULTS AND DISCUSSION

Genome Sequence Analysis of C. glutamicum for STPKs Encoding Genes—Examination of the *C. glutamicum* genome sequence revealed the presence of four putative genes encoding STPKs, all of which belong to the PKN2 family of prokaryotic protein kinases that are most closely related to the eukaryotic STPKs (27). To date, the corynebacterial STPKs have been

characterized to a limited extent. Only one of them, PknG, has been shown to participate in glutamine utilization (15), whereas the others (PknA, PknB, and PknL) remained uncharacterized. The genes encoding PknA and PknB are located, as in *M. tuberculosis* (16), in an apparent five-gene operon (*pstP, rodA, pbp2B, pknA,* and *pknB*). This operon is present in all corynebacterial genomes already sequenced (14, 28–30). The gene encoding PknL is present in the vicinity (6–8 kb) of the division and cell wall cluster comprising essential genes for cell division (*ftsQ* and *ftsZ*) and PG biosynthesis (*ftsI*, *murE*, *murF*, *mraY*, *murD*, *ftsW*, *murG*, and *murC*). PknL is in the opposite direction to the division and cell wall cluster, not only in corynebacteria, but also in other actinomycetes including *M. tuberculosis* (31, 32) and *Streptomyces coelicolor* (33). The gene encoding PknG is also located in a three-gene operon (*glnX, glnH*, and *pknG*) in all corynebacterial strains sequenced and, as mentioned above, is involved in glutamine utilization (15). Therefore, it seems essential to pursue the previous studies realized on the PknG kinase and also to newly characterize PknA, PknB, and PknL to extend our understanding of the role of corynebacterial STPKs.

Expression and Purification of the C. glutamicum STPKs—The *pknA*, *pknB*, *pknL*, and *pknG* genes encode 469-, 646-, 740-, and 822-amino acid proteins, with calculated molecular masses of 50, 68, 79, and 91 kDa, respectively. Primary sequence analysis revealed the presence of all the essential amino acids and sequence subdomains characterizing the Hanks' family of eukaryotic like protein kinases (34). These include the central core of the catalytic loop, consisting of subdomain VI, and the invariant lysine residue in the consensus motif within subdomain II, which is usually involved in the phosphotransfer reaction and required for the autophosphorylating activity of eukaryotic STPKs (Fig. 1) (34, 35). The hydropathy profiles of PknA, PknB, and PknL predict the presence of a single putative transmembrane constituting a membrane anchor (Fig. 2) (36). This transmembrane domain is lacking in PknG, which is a so-called cytoplasmic STPK. The extracellular portion of STPKs normally consists of one or more sensor domains that, when bound to their ligand, leads to intracellular conformational changes, which subsequently activate a signaling cascade. In some cases, this extracellular domain has been shown to possess penicillin-binding protein and serine/threonine kinase-associated (PASTA) motifs (37). In *M. tuberculosis* PknB, for instance, the extracellular portion contains four PASTA motifs, strongly supportive of a signal-binding sensor domain (38). This feature is also conserved in *C. glutamicum* PknB, which possesses three PASTA motifs (Fig. 2). Analysis of the *C. glutamicum* PknL primary sequence also predicts the presence of four PASTA motifs (Fig. 2), in contrast to *M. tuberculosis* PknL, which lacks the extracellular domain (31). This may implies that *C. glutamicum* PknL responds to different types of ligands than its myobacterial homologue.

To allow detailed biochemical studies, we focused our attention on the N-terminal cytoplasmic domains of PknA, PknB, and PknL corresponding to residues 1–332 out of 469, residues 1–313 out of 646, and residues 1–396 out of 740, respectively, comprising the kinase domain as well as the juxtamembrane linker (Fig. 2). The truncated genes lacking the DNA segments coding the hydrophobic C-terminal domain were synthesized by PCR amplification using genomic DNA from *C. glutamicum* ATCC 13869. The amplified products were cloned into plasmid pGEX4T-3, thus giving rise to pGEXA, pGEXB, and pGEXL. The recombinant GST-tagged $PknA_{CD}$, $PknB_{CD}$, and $PknL_{CD}$ fusion proteins were expressed in *E. coli* and purified using a glutathione-Sepharose 4B matrix. Analysis of the GST chimeric proteins by SDS-PAGE revealed that the wild-type enzymes were expressed in a soluble form and migrated with their predicted molecular masses, but also showed the presence of extra bands (Fig. 3*A*, *upper panel*). All these bands were analyzed by mass spectrometry, which confirmed the identity of the GST chimeric proteins (data not shown). An aberrant migration property has been observed previously for *M. tuberculosis* kinases, such as PknD, PknE, PknL, and PknH (20, 31, 39, 40), as well as for Pkn9 and Pkn6, two *Myxococcus xanthus* STPKs (41, 42). It was demonstrated that this specific pattern of migration was because of the different phosphorylated isoforms. Taken together, these results indicate that $PknA_{CD}$, $PknB_{CD}$, and $PknL_{CD}$ were produced as different soluble isoforms.

The full-length *pknG* gene (Fig. 2) was PCR-amplified using genomic DNA from *C. glutamicum* ATCC 13869. The product was cloned into plasmid pETTev, yielding to pTEVGfull. The recombinant His-tagged PknG protein was purified from *E. coli* using a Ni-NTA matrix. Analysis of the electrophoretic mobility of the protein by SDS-PAGE revealed that PknG was expressed in a soluble form according to its predicted molecular mass (Fig. 3*A*, *upper panel*).

Protein Kinase Activity of C. glutamicum STPKs—To investigate whether PknG, $PknA_{CD}$, $PknB_{CD}$, and $PknL_{CD}$ display autokinase activity, the purified kinases were incubated individually with [γ-^{33}P]ATP as a phosphate donor, separated by SDS-PAGE, and exposed to a x-ray film. As shown in Fig. 3*A* (*lower panel*), $PknA_{CD}$, $PknB_{CD}$, and $PknL_{CD}$ incorporated radioactive phosphate from [γ-^{33}P]ATP, generating a radioactive signal corresponding to the expected size of the protein isoforms, clearly indicating that these kinases undergo autophosphorylation. Unexpectedly, and in sharp contrast with $PknA_{CD}$, $PknB_{CD}$, or $PknL_{CD}$, PknG was not able to incorporate [γ-^{33}P]ATP (Fig. 3*A*, *lower panel*). To exclude the possibility that, in the full-length PknG protein, the C-terminal sensor domain could inhibit autophosphorylation activity, the PknG kinase domain alone was expressed, purified, and tested *in vitro* using [γ-^{33}P]ATP. No restoration of autophosphorylation activity could be detected, ruling out the hypothesis that the sensor domain exerts an inhibitory activity on PknG (data not shown).

Altogether, these data indicate that the N-terminal cytoplasmic domains of PknA, PknB, and PknL possess intrinsic autophosphorylation activity *in vitro*, whereas neither the kinase domain of PknG nor the full-length cytoplasmic protein showed autokinase activity. This prompted us to investigate whether cross-regulation/interaction between the PknG and PknA/B/L could occur.

Activation of PknG Phosphorylation Is Dependent on a PknA Cascade—In an elegant study, Kang *et al.* (16) demonstrated efficient intermolecular phosphorylation between PknA and PknB from *M. tuberculosis*, suggesting the possi-

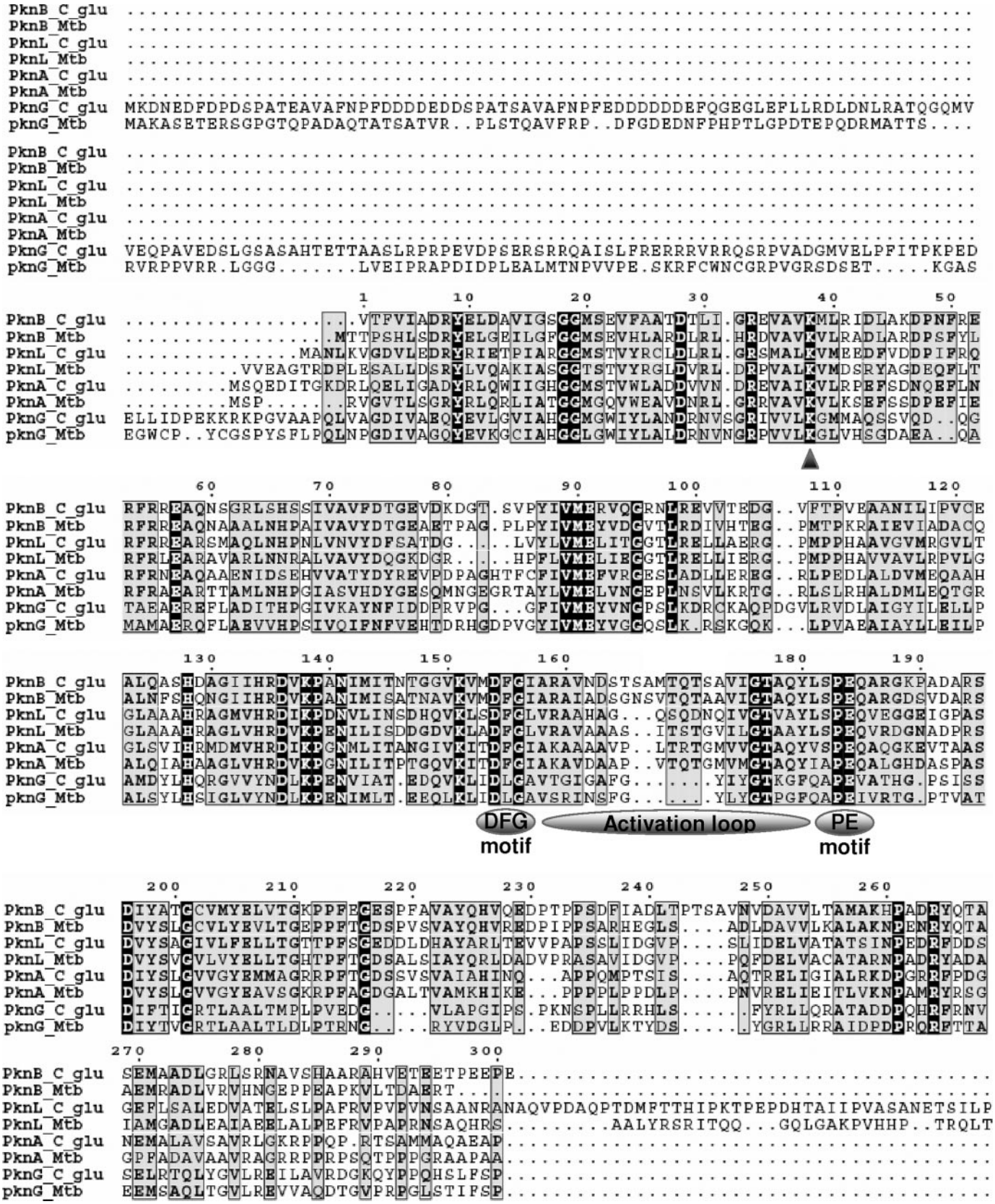

FIGURE 1. **Multiple sequence alignment of the kinase domains of *C. glutamicum* STPKs with their respective *M. tuberculosis* homologues.** The alignment was performed using ClustalW and Espript programs (*C_glu*, *C. glutamicum*; *Mtb*, *M. tuberculosis*). The conserved activation loop of the STPK family, delimited by the DFG and PE motifs, is represented by *shaded circles*. The key lysine residue involved in binding ATP is indicated by a *black triangle.*

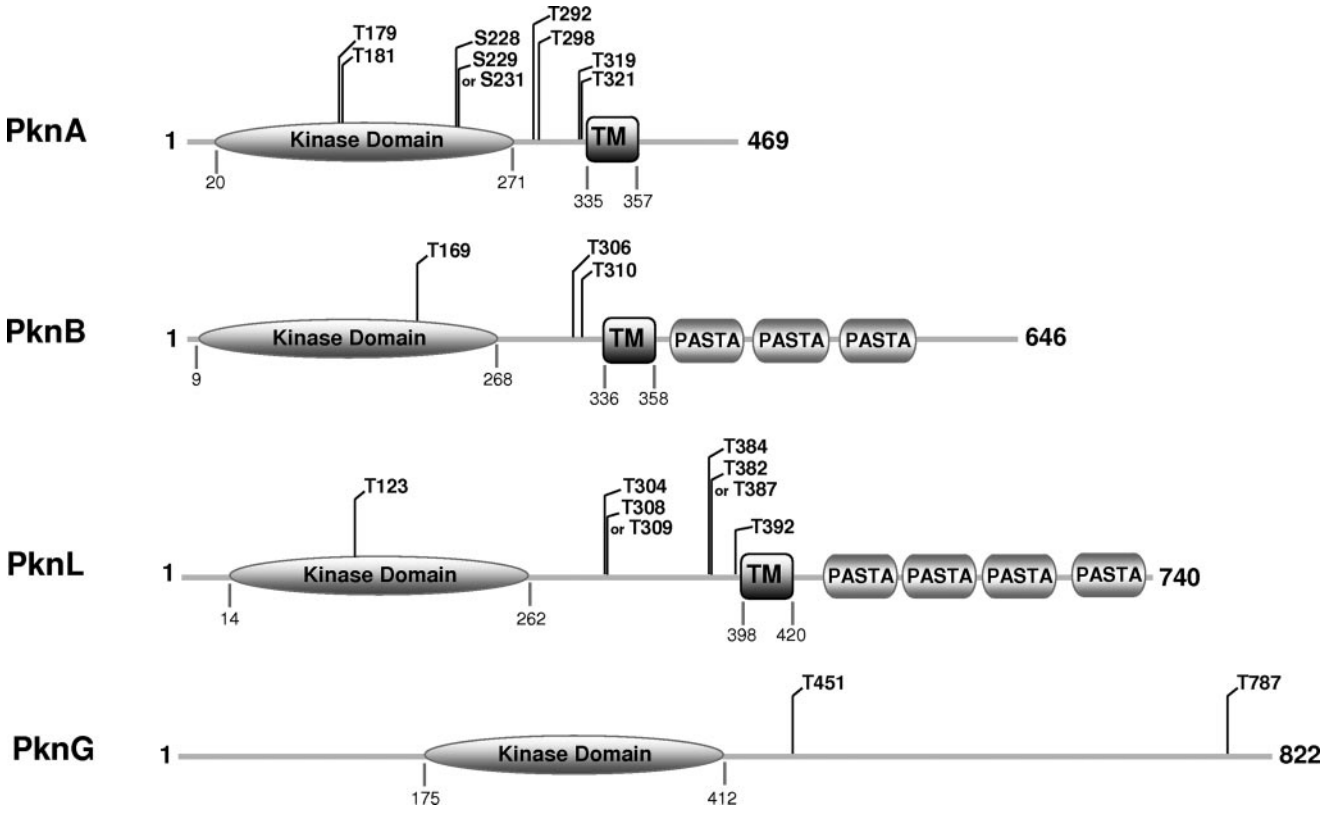

FIGURE 2. **Phosphorylated residues in the cytoplasmic domains of the four *C. glutamicum* STPKs.** The kinase domains and putative transmembrane regions (*TM*) are shown by *shaded circles* and *shaded boxes*, respectively. The extracellular PASTA motifs are represented by *different blocks*. Refer to Table 3 for further details.

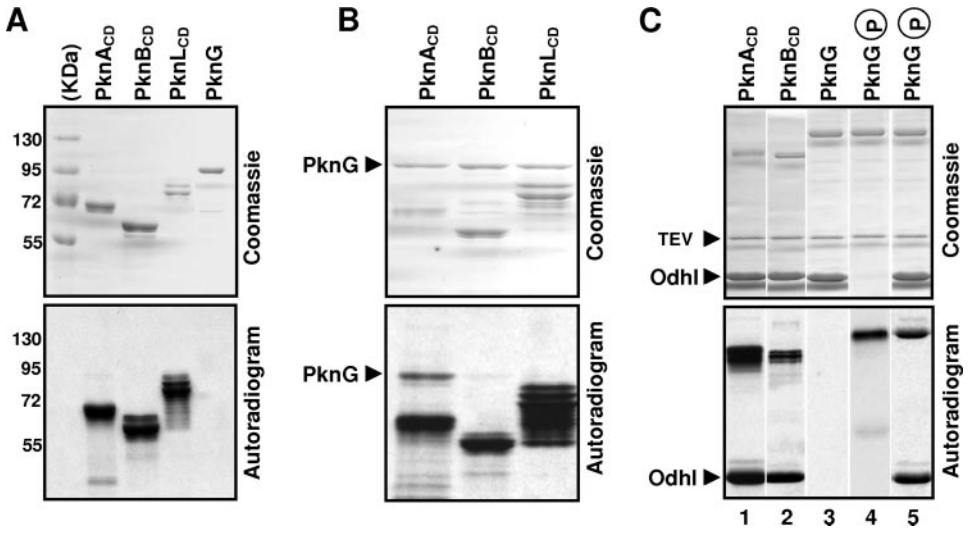

FIGURE 3. ***In vitro* phosphorylation activity of *C. glutamicum* STPKs.** *A,* cytoplasmic domains (*CD*) of PknA, PknB, and PknL proteins were overproduced and purified on glutathione-Sepharose 4B matrix. The full-length protein PknG was overproduced and purified on Ni-NTA matrix. The different kinases were submitted to gel electrophoresis and stained with Coomassie Blue (*upper panel*). *In vitro* phosphorylation assays were performed with [γ-^{33}P]ATP for 30 min. Proteins were analyzed by SDS-PAGE, and radioactive bands were revealed by autoradiography (*lower panel*). Standard proteins of known molecular masses were run in parallel (*kDa lane*). *B, in vitro* phosphorylation of PknG with PknA$_{CD}$, PknB$_{CD}$, and PknL$_{CD}$ was assayed with [γ-^{33}P]ATP for 30 min. Proteins were analyzed by SDS-PAGE and stained with Coomassie Blue (*upper panel*), and radioactive bands were revealed by autoradiography (*lower panel*). *C, in vitro* transphosphorylation of OdhI by PknA$_{CD}$, PknB$_{CD}$, or PknG was assayed with [γ-^{33}P]ATP for 30 min. Recombinant OdhI was treated with the TEV protease to remove the N-terminal His tag and used in phosphorylation assays in the presence of [γ-^{33}P]ATP: PknA$_{CD}$ and OdhI (*lane 1*), PknB$_{CD}$ and OdhI (*lane 2*), PknG and OdhI (*lane 3*), PknG after on-column phosphorylation by PknA (*lane 4*), and PknG after on-column phosphorylation by PknA and OdhI (*lane 5*). Proteins were separated by SDS-PAGE and stained with Coomassie Blue (*upper panel*), and radioactive bands were revealed by autoradiography (*lower panel*).

bility that cross-phosphorylation between these kinases may occur during signal transduction *in vivo*. This was demonstrated by assessing the ability of these kinases to phosphorylate each other, the wild-type form of one kinase mixed with the kinase-inactive form of the other (16).

We therefore reasoned that PknG may represent a substrate of PknA/B/L and that activation of PknG requires the protein to be phosphorylated by the other kinases. To test this hypothesis, His-tagged PknG was incubated with either PknA$_{CD}$, PknB$_{CD}$, or PknL$_{CD}$ in the presence of [γ-^{33}P]ATP. As shown in Fig. 3*B*, PknA was able to phosphorylate PknG. This supports the notion that intermolecular phosphorylation between PknA and PknG occurs and therefore may be part of a complex phosphorylation cascade. However, in a recent study, Niebisch *et al.* (15) provided evidence that purified Strep-tagged PknG catalyzed autophosphorylation and transphosphorylation activity to its

specific substrate 2-oxoglutarate dehydrogenase inhibitor protein (OdhI). OdhI is a 15-kDa protein with a ForkHead-associated domain and a homologue of mycobacterial GarA. One possible explanation of the discrepancy between the two studies may rely on the origin of the PknG used. In their study, Niebisch *et al.* (15) utilized a kinase that was overexpressed and purified from *C. glutamicum,* whereas we used an *E. coli* recombinant PknG protein. It is very likely that PknG from *C. glutamicum* had already been phosphorylated *in vivo* by other kinases, presumably PknA and "activated" to recognize and phosphorylate OdhI *in vitro*. However, whether PknG is phosphorylated by either PknA, PknB, or both PknA/B *in vivo* remains challenging, because null mutants of either *pknA* or *pknB* are lethal (see below), thus rendering an analysis of the individual contribution of these two kinases in phosphorylating PknG extremely difficult.

It is noteworthy that a scenario where a kinase is part of complex signaling cascade involving other kinases has been reported earlier in *M. xanthus* where Pkn8, a membrane-associated STPK, phosphorylates Pkn14, a cytoplasmic STPK. This latter phosphorylates MrpC on Thr residues, a transcriptional regulator essential for *M. xanthus* development (43).

We next cloned, overexpressed, and purified the *C. glutamicum* OdhI protein from *E. coli* and used it in *in vitro* phosphorylation assays. OdhI was purified as a His-tagged protein, which was expressed in soluble from and migrated as a 15-kDa protein as judged by Coomassie Blue staining after separation by SDS-PAGE (Fig. 3*C*, *upper panel*). In a first set of experiments, aimed to delineate the network of interactions between PknA, PknB, PknG, and OdhI, we analyzed whether OdhI could serve as a substrate. Fig. 3*C* (*lower panel*) clearly shows that, unlike PknA or PknB (*lanes 1* and *2*), PknG was unable to phosphorylate OdhI (*lane 3*). In another set of experiments, we tested whether PknA-dependent phosphorylation of PknG (allowing activation of PknG) would allocate PknG to phosphorylate OdhI. Because PknG was expressed as a His-tagged protein and PknA as a GST fusion protein, the different tags allowed us to selectively resolve one kinase from the other. The Ni-NTA resin-bound PknG was incubated with [γ-^{33}P]ATP and purified GST-PknA, thus allowing phosphorylation of the PknG kinase to occur. The Ni-NTA resin was extensively washed to eliminate the excess of unbound GST-PknA. Following elution from the Ni-NTA matrix, phosphorylated PknG was assayed *in vitro* with [γ-^{33}P]ATP supplemented or not with OdhI (Fig. 3*C*, *lanes 4* and *5*). PknG could be efficiently phosphorylated by PknA (Fig. 3*C*, *lane 4*) and, because of the absence of radioactive signal corresponding to the appropriate size of GST-PknA, one can ruled out the possibility of PknA contamination in the assay. The results indicate that PknG is required to be phosphorylated by PknA to efficiently transphosphorylate OdhI *in vitro* (Fig. 3*C*, *lane 5*). Overall, these findings are consistent with the hypothesis that PknG is dependent on PknA phosphorylation prior to phosphorylation of its specific substrate OdhI.

It is tempting to speculate that, *in vivo*, the PknA cascade is used to phosphorylate PknG, which in turn controls the 2-oxoglutarate dehydrogenase complex activity, a key enzyme of the tricarboxylic acid cycle, via the phosphorylation status of the PknG substrate, the OdhI regulator protein (15). This mechanism is of particular importance for the biotechnology production of about 1.5 million tons/year of L-glutamate by coryneform bacteria, where attenuation of 2-oxoglutarate dehydrogenase activity was found to be the key factor in the metabolic network (44). Furthermore, considering that the proteins PknG, OdhI (named as GarA in *M. tuberculosis*), and the 2-oxoglutarate dehydrogenase (OdhA) are highly conserved between *C. glutamicum* and *M. tuberculosis*, the signaling cascade involving these proteins could be similar in mycobacteria. This assumption is supported by the fact that the intracellular glutamate/glutamine level measured in an *M. tuberculosis* Δ*pknG* strain is increased (45). However, the *M. tuberculosis* PknG kinase purified from *E. coli* was capable of autophosphorylation activity *in vitro* (46), thus indicating that these kinases could possess a different mechanism of activation/regulation in the two microorganisms. It is noteworthy that *M. tuberculosis* possesses 11 STPKs compared with only 4 in *C. glutamicum*; therefore, the mechanism of regulation could be slightly different because of the possibility of an important STPK cross-talk in *M. tuberculosis*. Although the OdhI homologue in *M. tuberculosis*, GarA, was originally found to be phosphorylated by PknB (47), it is possible that a regulation mechanism, including PknA, PknG, and GarA, occurs in *M. tuberculosis*, similarly to what happens in *C. glutamicum*. Overall, these results led us to hypothesize that, *in vivo*, PknG from *C. glutamicum* could be part of a phosphorylation cascade, which in turns activates its kinase activity to control the 2-oxoglutarate dehydrogenase complex. Whether the STPK cross-talk occurs *in vivo* in *C. glutamicum* remains to be established, however. Further studies are currently under way to characterize more precisely the phosphorylation network in *C. glutamicum*, which also requires the identification of the phosphorylation sites of the kinases.

Identification of the $PknA_{CD}$, $PknB_{CD}$, $PknL_{CD}$, and PknG Phosphorylation Sites—Characterization of the phosphorylation sites in proteins provides a powerful tool to study signal transduction pathways and to decipher interaction networks involving signaling elements and is therefore of high biological relevance. Thus, assignment of the phosphorylation sites in STPKs is a major challenge in proteomics, particularly because some of these *C. glutamicum* STPKs may be involved in cell division (PknA, PknB, and PknL) or in regulation of the tricarboxylic acid cycle (PknG). A mass spectrometry approach was therefore used to identify the phosphoresidues in all four *C. glutamicum* STPKs. This technique has recently been proven to be the method of choice for characterizing post-translational modifications such as phosphorylation (31, 48). NanoLC/nanospray/tandem mass spectrometry was applied for the identification of phosphorylated peptides and for localization of phosphorylation sites in the different kinases. Purified GST-$PknA_{CD}$, GST-$PknB_{CD}$, or GST-$PknL_{CD}$ was subjected to *in vitro* phosphorylation with nonradioactive ATP, whereas His-tagged PknG was phosphorylated with PknA and nonradioactive ATP prior to resolving on SDS-PAGE and in-gel digestion with either trypsin or chymotrypsin. Peptides deriving from $PknA_{CD}$, $PknB_{CD}$, $PknL_{CD}$, or PknG were identified by nanoLC/nanospray/MS/MS, which led to 90, 90, 80, and 80% of

TABLE 3
Phosphorylation status of recombinant protein kinases $PknA_{CD}$, $PknB_{CD}$, $PknL_{CD}$, and PknG as determined by mass spectrometry

Phosphorylated tryptic and chymotryptic peptide sequence	Number of detected phosphate groups, LC-ESI/MS/MS[a]	Phosphorylated residue(s)
$PknA_{CD}$		
^{172}AAAAVPL**T**R^{180}	1	Thr-179
^{172}AAAAVPL**T**RTGMVVGTAQYVSPEQAQGK^{199}	1	Thr-179
^{172}AAAAVPL**T**R**T**GMVVGTAQYVSPEQAQGK^{199}	2	Thr-179 and Thr-181
^{168}GIAKAAAAVPL**T**R**T**GMVVGTAQY^{190}	2	Thr-179 and Thr-181
^{222}RPFTGD**S**S**V**S**V**AIAHINQAPPQMPTSISAQTR^{253}	1	Ser-228 or Ser-229 or Ser-231
^{222}RPFTGD**S**S**V**S**V**AIAHINQAPPQMPTSISAQTR^{253}	2	Ser-228 and Ser-229 or Ser-231
^{225}TGD**S**S**V**S**V**AIAH^{236}	1	Ser-228
^{283}LGKRPPQPR**T**SAMMAQAEAPSPSES**T**AMLGR^{313}	2	Thr-292 and Thr-298
^{314}VARPA**T**I**T**QEAAPK^{327}	1	Thr-319
^{314}VARPA**T**I**T**QEAAPK^{327}	2	Thr-319 and Thr-321
^{314}VARPA**T**I**T**QEAAPK^{327}	1	Thr-321
^{317}PA**T**I**T**QEAAPK^{327}	2	Thr-319 and Thr-321
$PknB_{CD}$		
^{160}AVNDSTSAM**T**QTSAVIGTAQYLSPEQAR^{187}	1	Thr-169
^{304}FS**T**RTSTQVA^{313}	1	Thr-306
^{304}FS**T**RTS**T**QVA^{313}	2	Thr-306 and Thr-310
$PknL_{CD}$		
^{120}GVL**T**GLAAAHR^{130}	1	Thr-123
^{294}ANAQVPDAQP**T**DMF**T**T**H**IPK^{313}	2	Thr-304 and (Thr-308 or Thr-309)
^{366}NIQDQELARADEPEIN**T**VSNRSKL^{389}	1	Thr-382
^{375}ADEPEIN**T**VSNR^{386}	1	Thr-382
^{375}ADEPEIN**T**V**S**NR**S**K^{388}	2	Thr-382 and Ser-384 or Ser-387
^{389}LKL**T**LWSI^{396}	1	Thr-392
^{387}SKLKL**T**LWSI^{396}	1	Thr-392
PknG		
^{447}STFG**T**KHLVFR^{457}	1	Thr-451
^{450}G**T**KHLVF^{456}	1	Thr-451
^{784}GLR**T**GISEALR^{794}	1	Thr-787
^{782}SKGLR**T**GISEALR^{794}	1	Thr-787

[a] LC-ESI/MS/MS is nanoLC/nanospray/tandem mass spectrometry.

sequence coverage, respectively. Therefore, one cannot exclude the possibility of additional phosphorylated serine or threonine residues not covered by this analysis. Phosphorylated amino acid residues were assigned by peptide fragmentation in MS/MS; *y* and *b* daughter ions containing one phosphoserine or phosphothreonine were associated with a neutral loss of phosphoric acid ($-H_3PO_4$, *i.e.* −98 Da).

As detailed in Table 3, and presented in Fig. 2, analysis of tryptic and chymotryptic digests allowed the characterization of 8, 3, 6, and 2 phosphorylation sites in $PknA_{CD}$, $PknB_{CD}$, $PknL_{CD}$, and PknG, respectively. PknB from *M. tuberculosis*, one of the most studied mycobacterial STPK, possesses the two characteristic threonines in its activation loop (Thr-171 and Thr-173) (38), whereas two other *M. tuberculosis* kinases, PknE and PknH, only harbor a single Thr residue (49). Mass spectrometric profiling of the *C. glutamicum* STPKs phosphorylation sites indicated that PknA contains two phosphorylated Thr residues (Thr-179 and Thr-181) present in the activation loop. The corynebacterial PknB possesses one phosphorylated Thr (Thr-169) within its activation loop instead of two in its *M. tuberculosis* counterpart (Fig. 1 and Fig. 2). However, one cannot exclude the possibility that the Thr-171 was missed in our analysis. Together, these results suggest that the corynebacterial PknA and PknB enzymes present a classical mechanism of activation via the activation loop.

Surprisingly, unlike all the other kinases, PknL from *C. glutamicum* does not possess a classical T*X*T activation loop motif (Fig. 1). The TST motif found in *M. tuberculosis* PknL (31) is replaced by an SQD motif in *C. glutamicum* PknL. This was rather unexpected because PknL still undergoes autophosphorylation. These important differences may reflect mechanistic differences of activation/regulation of PknL in the two microorganisms. Therefore, differential structure organizations (PknL possessing an extracytoplasmic region in *C. glutamicum*, which is not conserved in *M. tuberculosis*) may account for these mechanistic differences.

Concerning PknG, this kinase presents a completely different structural organization as being a cytoplasmic protein with no transmembrane region but still harboring a classical kinase domain. No phosphorylated residue could be identified within the activation loop. In fact, this region is missing in the PknG kinase, in both *C. glutamicum* and *M. tuberculosis* (Fig. 1), thus pointing to an unusual mechanism of phosphorylation of this kinase. In addition, mass spectrometric profiling of the PknG phosphorylation sites not only confirmed that this kinase is phosphorylated by the PknA, but also identified two unique phosphorylation sites, Thr-451 and Thr-787 located in the C terminus of the enzyme.

Thus, mass spectrometry profiling coupled to *in vitro* kinase assays unambiguously demonstrated the Ser/Thr kinase activity of the four *C. glutamicum* kinases. From a general standpoint, this type of analysis provides an essential groundwork for mechanistic/functional studies of bacterial STPKs and demonstrates the efficiency of combining genetics and mass spectrometry analyses with precise identification of phosphoacceptors, a prerequisite for a further understanding of the mode of action of PknA, PknB, PknL, and PknG. In particular, strains with defined mutations within the phosphorylation sites will be extremely helpful to establish the role of these kinases in corynebacterial growth and physiology. Consequently, this characterization significantly contributes to increasing our understanding of the biological mechanisms that control cellu-

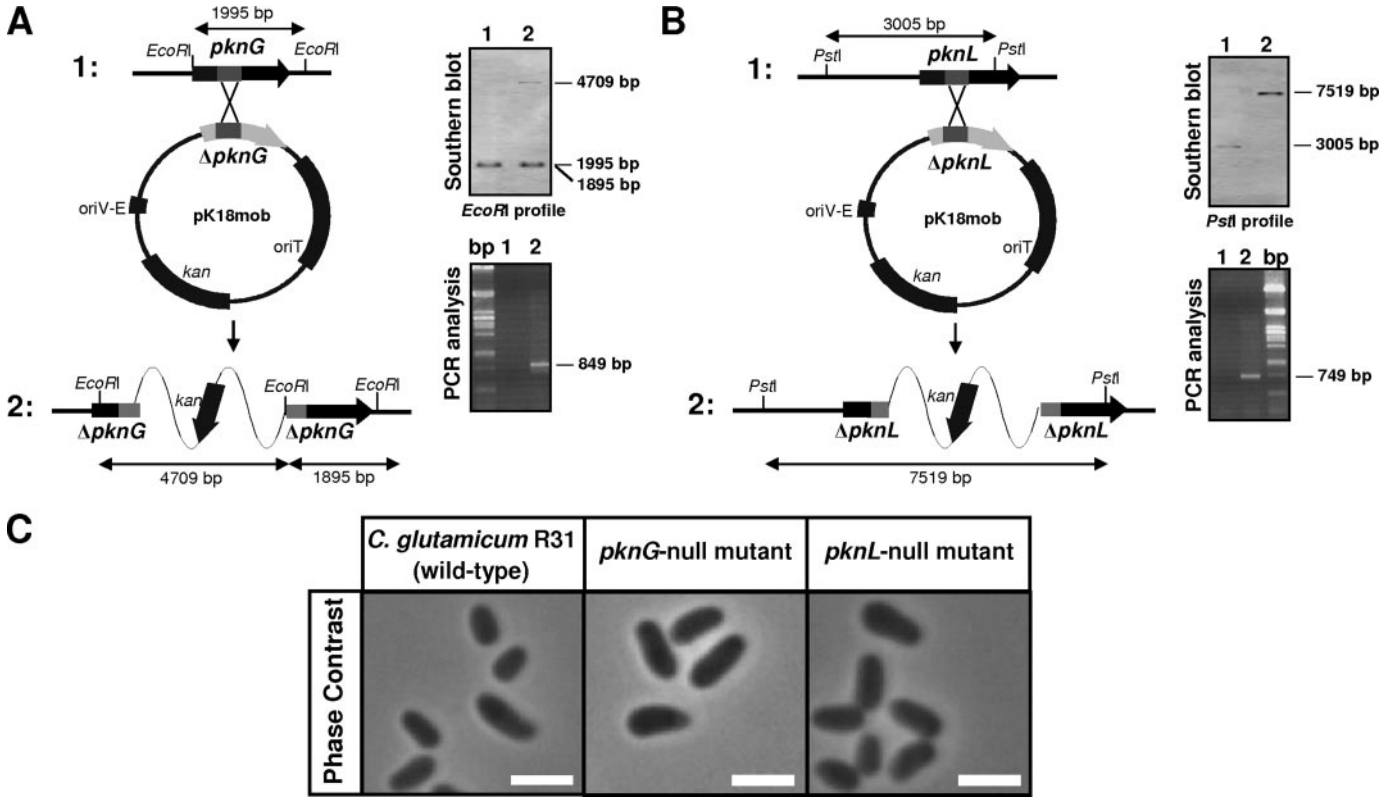

FIGURE 4. **Construction of *C. glutamicum pknG* and *pknL* null mutants.** *A,* schematic representation of the chromosomal region around *pknG* in *C. glutamicum* R31 (*1*) and in a *pknG* null mutant (*2*) obtained by integration of pKGint into the chromosome of R31. Southern blot analysis of EcoRI-digested chromosomal DNA from R31 (*lane 1*) and *pknG* null mutant (*lane 2*) using an internal fragment of the *pknG* gene as probe. PCR analysis was performed using total chromosomal DNA from R31 (*lane 1*) and *pknG* null mutant (*lane 2*) using primers M13–26 and pknGint2 (see Table 2). Size of the PCR fragments is represented in base pairs (*bp*). *B,* schematic representation of the chromosomal region around *pknL* in *C. glutamicum* R31 (*1*) and in a *pknL* null mutant (*2*) obtained by integration of pKLint into the chromosome of R31. Southern blot analysis of PstI-digested chromosomal DNA from R31 (*lane 1*) and *pknL* null mutant (*lane 2*) using an internal fragment of the *pknL* gene as probe. PCR analysis was performed using total chromosomal DNA from R31 (*lane*) and *pknL* null mutant (*lane 2*) using primers M13–26 and pknLint2 (see Table 2). Size of the PCR fragments is represent in base pairs (*bp*). *C,* microscopic images of *pknG* and *pknL* null mutants of *C. glutamicum*. Cells were observed in a Nikon E400 by phase contrast microscopy. The typical morphology of *C. glutamicum* R31 was conserved in strains deleted in *pknG* or *pknL*. *Size bar,* 1 μm.

lar processes and cell regulation in this major industrial bacterial producer. In addition, characterization of these kinases should also help in examining their potential role in pathogenicity of the virulent species *Corynebacterium diphtheriae,* in which the four kinases are conserved (data not shown) (29).

Inactivation of pknA, pknB, pknL, and pknG in C. glutamicum—To further characterize the role of these kinases *in vivo*, and to appreciate the extent to which they are required for growth and viability of *C. glutamicum*, the corresponding chromosomal genes were inactivated using a previously described method (50). Niebisch *et al.* (15) demonstrated that a Δ*pknG* mutant was unable to grow on minimal medium with glutamine as sole carbon and nitrogen source. Therefore, *pknG* is not essential for *C. glutamicum* growth in complex medium (15). Gene disruption was carried out using internal fragments of *pknA, pknB,* and *pknL*. The internal fragment of *pknG* was used as control because *pknG* was not essential for the viability of *C. glutamicum* in complex medium. The conjugative suicide plasmids pKAint, pKBint, pKGint, and pKLint (Table 1) were introduced separately into *E. coli* S17-1 and mated with *C. glutamicum* R31 cells. *C. glutamicum* kanamycin-resistant transconjugants could only be obtained after mating with *E. coli* [pKGint] and *E. coli* [pKLint] (Fig. 4). These results suggest that inactivation of *pknA* or *pknB* leads to cell death; hence the absence of *pknA* or *pknB* transconjugants is consistent with the conclusion that in *M. tuberculosis pknA* and *pknB* are essential genes (16, 51). However, the chromosomal *pknG* and *pknL* genes could be disrupted in the transconjugants *C. glutamicum* [pKGint] and *C. glutamicum* [pKLint]. Gene inactivation was confirmed by PCR analysis as well as by Southern blotting (Fig. 4, *A* and *B*). The *pknL* and *pknG* mutants showed a similar phenotype by phase contrast microscopy compared with the wild-type strain (Fig. 4*C*) and did not present any morphological alteration, suggesting that the *pknG* and *pknL* are not essential for viability at least in complex medium. Moreover, phenotype analysis of the corynebacterial strains overexpressing functional PknL or PknG did not reveal any differences compared with the wild-type control strain (data not shown).

Overall, our results suggest that the *C. glutamicum pknA* and *pknB* genes are essential, whereas the *pknL* and *pknG* genes are no longer necessary for growth. Thus, we focused our study on PknA and PknB, which appear to be key components of *C. glutamicum* growth and viability.

Partial Depletion of PknA or PknB Delays Growth and Produces Elongated Cells—Because PknA and PknB are essential, we were unable to examine the phenotypes of corynebacterial *pknA* or *pknB* null mutants. We therefore used a conditional expression system to reduce the amount of PknA or PknB in the

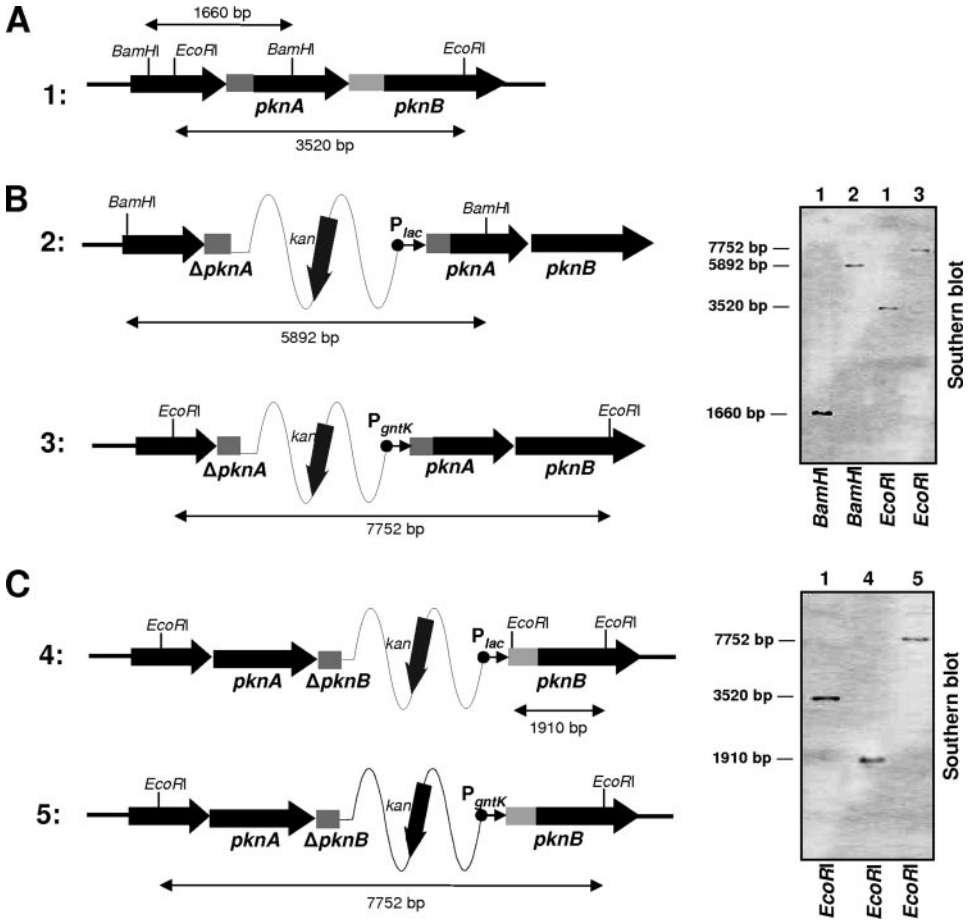

FIGURE 5. **Construction of *C. glutamicum pknA* and *pknB* conditional expression strains.** The suicide plasmids pKLA/B (P_{lac}-Δ*pknA/B*) and pKPKA/B (P_{gntK}-Δ*pknA/B*) were introduced into *C. glutamicum* by conjugation to disrupt the chromosomal copy of the gene and to introduce a functional copy of *pknA* or *pknB* under the control of the P_{lac} and P_{gntK} promoters, respectively. *A,* restriction map of the wild-type *pknA* and *pknB* locus (*1*). *B,* restriction maps of the P_{lac}-Δ*pknA locus* (*2*) and P_{gntK}-Δ*pknA* locus (*3*), respectively. Southern blot analysis of chromosomal DNA from P_{lac}-Δ*pknA* strain (*lane 2*) and P_{gntK}-Δ*pknA* strain (*lane 3*) digested with EcoRI or BamHI. The probe used was an internal fragment of the *pknA* gene. *C,* restriction maps of the P_{lac}-Δ*pknB locus* (*4*) and P_{gntK}-Δ*pknB* locus (*5*), respectively. Southern blot analysis of chromosomal DNA from P_{lac}-Δ*pknB* strain (*lane 4*) and P_{gntK}-Δ*pknB* strain (*lane 5*) digested with EcoRI. The probe used was an internal fragment of the *pknB* gene.

cells to investigate their function. To this purpose, *C. glutamicum* was conjugated with *E. coli* carrying the suicide plasmids pKLA/B (P_{lac}-Δ*pknA/B*) or pKPKA/B (P_{gntK}-Δ*pknA/B*) (Table 1). These plasmids were designed to disrupt the chromosomal copy of the gene and to introduce a functional copy of the *pknA* or *pknB* gene under the control of the P_{lac} and P_{gntK} promoters, respectively. The P_{gntK} promoter is located upstream of the *gntK* gene encoding the *C. glutamicum* gluconate kinase and is regulated by sucrose (2). The *E. coli* P_{lac} promoter allows low expression levels in *C. glutamicum* (52). In *C. glutamicum,* pKLA/B and pKPKA/B were unable to replicate autonomously but integrated by homologous recombination into the chromosomal *pknA/B* locus, respectively. This resulted in the disruption of the targeted gene under its native promoter and the introduction of a functional copy of the corresponding gene placed under the control of the heterologous promoters P_{lac} or P_{gntK} (Fig. 5). Southern blot analysis (Fig. 5) and PCR analysis (data not shown) confirmed the correct pattern expected for integration of plasmids pKLA/B and pKPKA/B at the chromosomal *pknA* or *pknB* loci in the *C. glutamicum* transconjugant strains.

C. glutamicum strains under-expressing *pknA* or *pknB* from either the P_{lac} or P_{gntK} promoters showed an elongated phenotype that was undoubtedly different from the rod-shaped cells of the control strain *C. glutamicum* R31 (Fig. 6). These elongated bacteria were twice or three times the size of the wild-type bacteria and also appeared wider. In an attempt to determine whether these strains depleted in PknA or PknB were affected in cell wall biosynthesis, the cells were stained with Van-FL. Van-FL staining is often used to visualize the incorporation of newly synthesized PG at the sites of nascent PG synthesis during cell division in Gram-positive bacteria (4) because it is known that Van-FL is able to bind to the terminal D-Ala-D-Ala of the lipid-linked PG precursor (53). Fig. 6 indicates that in the *C. glutamicum* R31 control strain the newly synthesized PG was incorporated both at the cell poles and at the septum as reported earlier (4). In contrast, Van-FL staining of strains depleted in either PknA or PknB indicated that active PG biosynthesis was taking place at the cell poles as well as in multiple septa presumably corresponding to multiple division sites within the elongated *C. glutamicum* cells. This elongated phenotype could be the consequence of an error/defect in the cell division process probably linked to the reduced level of PknA/B.

In addition, in an attempt to determine whether these strains depleted in PknA or PknB were affected in DNA segregation, cells were stained with 4′-6-diamidino-2-phenylindole (DAPI), which is able to form fluorescent complexes with natural double-stranded DNA, thus providing a useful tool in cytochemical investigations, and especially to visualize nucleoids (25). DAPI staining of the PknA- or PknB-depleted strains showed the presence of multiple nucleoids (Fig. 6), synonymous of several DNA replication events and suggesting that DNA segregation took place properly but that the final steps of cell division were inhibited. Similar phenotypes were reported in *C. glutamicum* with altered levels of FtsZ (52) and PBP2b (50). Interestingly, FtsZ and PBPA (homologous to *C. glutamicum* PBP2b) from *M. tuberculosis* are also substrates of PknA and PknB, respectively (17, 18).

We also investigated whether these major phenotype changes could affect *C. glutamicum* growth and viability. Cell growth of a PknA-depleted strain (Fig. 7*A*) as well as a PknB-depleted strain (Fig. 7*B*) was clearly delayed, characterized by

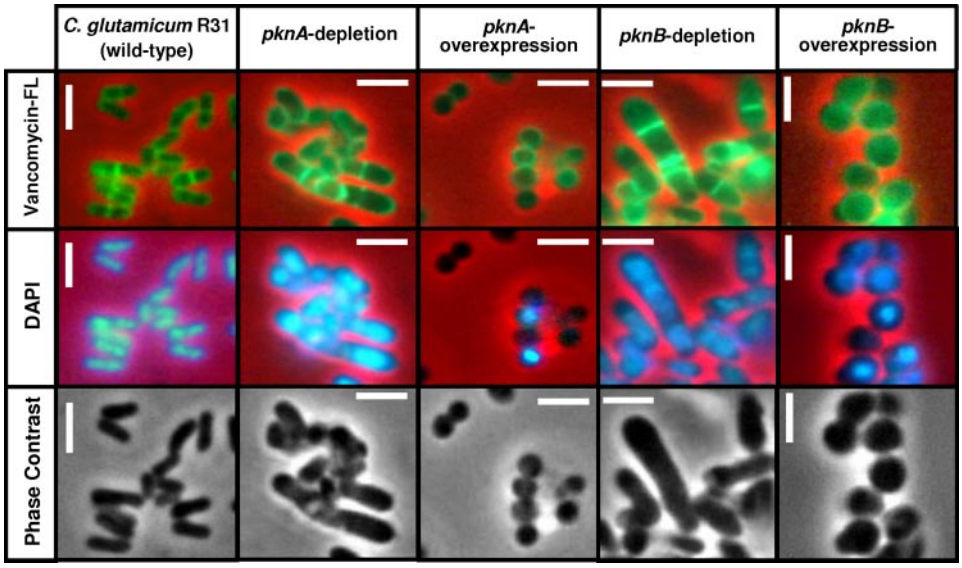

FIGURE 6. **Microscopy of *C. glutamicum* strains with conditional expression of PknA and PknB levels.** *C. glutamicum* cells were stained with vancomycin-FL or DAPI fluorescent dyes and observed using a Nikon E400 fluorescence microscope. The typical morphology of *C. glutamicum* R31 was converted to a coccoid morphology (no polar growth) in strains overexpressing *pknA* or *pknB*, whereas strain depleted for PknA or PknB grew apically and formed many apparently incomplete septa. Overlays of fluorescence images of vancomycin-FL (*green*) or DAPI (*blue*) are shown. Phase contrast images are also showed. *Size bar,* 1 μm.

A

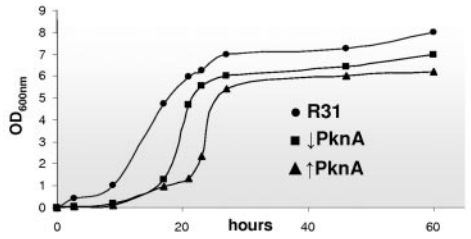

OD600nm	R31	↑ PknA	↓ PknA
1	$1.5x10^8$	$5.5x10^7$	$3.3x10^7$
3	$4.1x10^8$	$3.0x10^8$	$1.5x10^8$
6.1	$7.2x10^8$	$5.3x10^8$	$2.3x10^8$
7.8	$8.2x10^8$	$7.3x10^8$	$4.1x10^8$

B

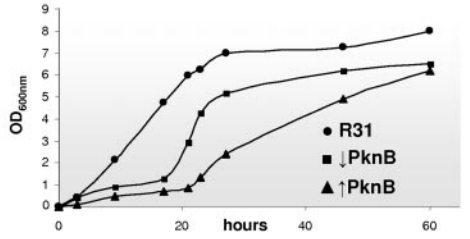

OD600nm	R31	↑ PknB	↓ PknB
1	$1.5x10^8$	$2.2x10^7$	$8.3x10^6$
3	$4.1x10^8$	$1.0x10^8$	$2.5x10^7$
6.1	$7.2x10^8$	$1.9x10^8$	$6.0x10^7$
7.8	$8.2x10^8$	$3.1x10^8$	$8.3x10^7$

FIGURE 7. **Growth and viability of *C. glutamicum* strains expressing different levels of the PknA and PknB kinases.** *A,* strains with different levels of PknA: normal (R31), reduced (↓), and increased (↑). *B,* strains with different levels of PknB: normal (R31), reduced (↓), and increased (↑). Viable bacterial counts are expressed as the number of colony counts per ml. Numbers are representative of three independent experiments.

an important lag phase. In addition, these strains showed markedly diminished viability with a more severe effect caused by depleting PknB (about a 10-fold decrease compared with the wild-type R31 strain) than PknA (Fig. 7, *A* and *B*). Overall, these data suggest that low expression levels of PknA or PknB profoundly alter cell division. This interpretation is supported by the localization of *pknA* and *pknB* in a gene cluster that includes *rodA* and *pbp2b*, genes encoding orthologues of proteins that are important in this cell division and cell wall biosynthesis in corynebacteria (14).

Overexpression of PknA or PknB Delays Growth and Results in a Coccoid Cell-shaped Phenotype—We next examined the phenotypic effects of overexpressing PknA or PknB in *C. glutamicum*. Both the PknA- and the PknB-overexpressing strains were characterized by a delayed growth rate with a slightly diminished viability than did the control R31 strain (Fig. 7, *A* and *B*), consistent with the results obtained in *M. smegmatis* strains overexpressing the *M. tuberculosis pknA* or *pknB* genes (16). To observe the consequences of *pknA* or *pknB* overexpression on cell morphology, early exponential phase growing cells were harvested and examined microscopically. Interestingly, overexpression of either *pknA* or *pknB* leads to completely different morphotypes from those observed in the *pknA*- or *pknB*-depleted strains. Indeed, cells presented a characteristic coccoid-like phenotype compared with the control strain (Fig. 6). This particular cell shape suggests that cell elongation was strongly disturbed. In fact, Van-FL staining revealed incorporation of nascent PG around the cells indicating a lack of polar PG synthesis (Fig. 6). In addition, *C. glutamicum* cells overexpressing PknA or PknB form chains of cells attached at the poles, as seen for streptococci (54), suggesting a possible role of PknA and PknB in the final stages of cell division or cell-pole maturation.

In addition, DAPI staining highlights the fact that an important proportion of the cells overexpressing *pknA* or *pknB* was lacking detectable DNA, pointing to either a lack of chromosome segregation control (24) or to an indirect effect of the lack of polarization in the coccoid cells, which could be responsible for a DNA segregation problem (55, 56). This coccoid-like phenotype was rather unexpected, as it was not observed in mycobacterial strains overexpressing the *M. tuberculosis pknA* or *pknB* genes (16). Although the effects on cell morphology are strongly supportive of a function of PknA and PknB kinases in the regulation of the cell shape and morphology in corynebacteria and mycobacteria, these results also suggest that the mechanisms, or the substrates, involved in these processes are different in the two organisms. For instance, Wag31, the *M. tuberculosis* homologue of the corynebacterial cell division protein DivIVA, a key protein that regulates growth, morphology, and polar cell wall synthesis, is phosphorylated by *M. tuberculosis* PknA and PknB (57). Thus, we have tested the ability of the *C. glutamicum* DivIVA protein to be a substrate of the four corynebacterial STPKs *in vitro* but failed to detect any phosphorylation (data not shown). Wag31 and DivIVA have two predicted coiled-coil regions that are inter-

rupted by a highly variable sequence (58). Interestingly, this highly variable sequence contains the unique phosphorylated site in mycobacterial Wag31 (Thr-73), which is not conserved in the *C. glutamicum* DivIVA protein (data not shown). This illustrates the fact that signal transduction pathways mediated by kinases for the regulation of cell shape in corynebacteria are likely to be different from mycobacteria. Our experimental data, along with previous work (16, 38, 47, 57, 59), strongly support a consistency of function of the PknB-like kinases in regulating cell shape and growth in a broad range of Gram-positive microorganisms.

In conclusion, our results provide, for the first time, a biochemical and comparative analysis of all four STPKs and the involvement of PknA and PknB in a signaling pathway in the process of cell shape control and cell division in corynebacteria. Our study also delineates important differences with the mycobacterial homologous kinases. In particular, we provided evidence that corynebacterial PknG, but not mycobacterial PknG, requires phosphorylation by PknA prior to transphosphorylation of its substrate OdhI. This suggests that, in addition to PknG, PknA may also participate in the phosphorylation status of OdhI and as a consequence, in the control of 2-oxoglutarate dehydrogenase, a key enzyme of the tricarboxylic acid cycle. A proteomic study revealed the presence of an important number of phosphorylated proteins in *C. glutamicum*, with the vast majority being metabolic enzymes rather than regulatory proteins, suggesting that protein phosphorylation plays a much broader function in the physiology of the bacteria than was previously expected (60). Therefore, further work needs to be carried out to understand how the limited number of kinases recognize an important number of substrates and how they participate in many complex signaling pathways. Another perspective of this work is the opening of a new field of investigation for future drug development to combat pathogenic corynebacterial species, such as *C. diphtheriae* or emerging corynebacterial pathogens. Because both PknA and PknB are essential, specific inhibitors capable of preventing corynebacterial growth would be extremely useful for the development of new therapies. In this context, recent studies demonstrated that mitoxantrone, a compound used in cancer treatment, represents a valid PknB inhibitor capable of preventing *M. tuberculosis* growth, suggesting that bacterial kinases represent a potential target for drug design (61). Whether mitoxantrone also inhibits corynebacterial growth remains to be established.

REFERENCES

1. Hermann, T. (2003) *J. Biotechnol.* **104,** 155–172
2. Letek, M., Valbuena, N., Ramos, A., Ordonez, E., Gil, J. A., and Mateos, L. M. (2006) *J. Bacteriol.* **188,** 409–423
3. Letek, M., Ordonez, E., Fiuza, M., Honrubia-Marcos, P., Vaquera, J., Gil, J. A., Castro, D., and Mateos, L. M. (2007) *Int. Microbiol.* **10,** 271–282
4. Daniel, R. A., and Errington, J. (2003) *Cell* **113,** 767–776
5. Letek, M., Ordonez, E., Vaquera, J., Margolin, W., Flardh, K., Mateos, L. M., and Gil, J. A. (2008) *J. Bacteriol.* **190,** 3283–3292
6. Scheffers, D. J., Jones, L. J., and Errington, J. (2004) *Mol. Microbiol.* **51,** 749–764
7. Munoz-Dorado, J., Inouye, S., and Inouye, M. (1991) *Cell* **67,** 995–1006
8. Zhang, W., Munoz-Dorado, J., Inouye, M., and Inouye, S. (1992) *J. Bacteriol.* **174,** 5450–5453
9. Shi, L., Potts, M., and Kennelly, P. J. (1998) *FEMS Microbiol. Rev.* **22,** 229–253
10. Grangeasse, C., Cozzone, A. J., Deutscher, J., and Mijakovic, I. (2007) *Trends Biochem. Sci.* **32,** 86–94
11. Stock, A. M., Robinson, V. L., and Goudreau, P. N. (2000) *Annu. Rev. Biochem.* **69,** 183–215
12. Narayan, A., Sachdeva, P., Sharma, K., Saini, A. K., Tyagi, A. K., and Singh, Y. (2007) *Physiol. Genomics* **29,** 66–75
13. Hett, E. C., and Rubin, E. J. (2008) *Microbiol. Mol. Biol. Rev.* **72,** 126–156
14. Kalinowski, J., Bathe, B., Bartels, D., Bischoff, N., Bott, M., Burkovski, A., Dusch, N., Eggeling, L., Eikmanns, B. J., Gaigalat, L., Goesmann, A., Hartmann, M., Huthmacher, K., Kramer, R., Linke, B., McHardy, A. C., Meyer, F., Mockel, B., Pfefferle, W., Puhler, A., Rey, D. A., Ruckert, C., Rupp, O., Sahm, H., Wendisch, V. F., Wiegrabe, I., and Tauch, A. (2003) *J. Biotechnol.* **104,** 5–25
15. Niebisch, A., Kabus, A., Schultz, C., Weil, B., and Bott, M. (2006) *J. Biol. Chem.* **281,** 12300–12307
16. Kang, C. M., Abbott, D. W., Park, S. T., Dascher, C. C., Cantley, L. C., and Husson, R. N. (2005) *Genes Dev.* **19,** 1692–1704
17. Dasgupta, A., Datta, P., Kundu, M., and Basu, J. (2006) *Microbiology* **152,** 493–504
18. Thakur, M., and Chakraborti, P. K. (2006) *J. Biol. Chem.* **281,** 40107–40113
19. Mateos, L. M., Schafer, A., Kalinowski, J., Martin, J. F., and Puhler, A. (1996) *J. Bacteriol.* **178,** 5768–5775
20. Molle, V., Kremer, L., Girard-Blanc, C., Besra, G. S., Cozzone, A. J., and Prost, J. F. (2003) *Biochemistry* **42,** 15300–15309
21. Cohen-Gonsaud, M., Barthe, P., Pommier, F., Harris, R., Driscoll, P. C., Keep, N. H., and Roumestand, C. (2004) *J. Biomol. NMR* **30,** 373–374
22. Molle, V., Brown, A. K., Besra, G. S., Cozzone, A. J., and Kremer, L. (2006) *J. Biol. Chem.* **281,** 30094–30103
23. Kieser, T., Bibb, M. J., Buttner, M. J., Chen, B. F., and Hopwood, D. A. (2000) *Practical Streptomyces Genetics*, pp. 161–220, John Innes Institute, Norwich, UK
24. Letek, M., Fiuza, M., Ordonez, E., Villadaneos, A. F., Ranos, A., Mateos, L. M., and Gil, J. A. (2008) *Antonie Leeuwenhoek* 10.1007/S10482-008-9224-4
25. Daniel, R. A., Harry, E. J., and Errington, J. (2000) *Mol. Microbiol.* **35,** 299–311
26. Shevchenko, A., Wilm, M., Vorm, O., and Mann, M. (1996) *Anal. Chem.* **68,** 850–858
27. Leonard, C. J., Aravind, L., and Koonin, E. V. (1998) *Genome Res.* **8,** 1038–1047
28. Nishio, Y., Nakamura, Y., Kawarabayasi, Y., Usuda, Y., Kimura, E., Sugimoto, S., Matsui, K., Yamagishi, A., Kikuchi, H., Ikeo, K., and Gojobori, T. (2003) *Genome Res.* **13,** 1572–1579
29. Cerdeno-Tarraga, A. M., Efstratiou, A., Dover, L. G., Holden, M. T., Pallen, M., Bentley, S. D., Besra, G. S., Churcher, C., James, K. D., De Zoysa, A., Chillingworth, T., Cronin, A., Dowd, L., Feltwell, T., Hamlin, N., Holroyd, S., Jagels, K., Moule, S., Quail, M. A., Rabbinowitsch, E., Rutherford, K. M., Thomson, N. R., Unwin, L., Whitehead, S., Barrell, B. G., and Parkhill, J. (2003) *Nucleic Acids Res.* **31,** 6516–6523
30. Tauch, A., Kaiser, O., Hain, T., Goesmann, A., Weisshaar, B., Albersmeier, A., Bekel, T., Bischoff, N., Brune, I., Chakraborty, T., Kalinowski, J., Meyer, F., Rupp, O., Schneiker, S., Viehoever, P., and Puhler, A. (2005) *J. Bacteriol.* **187,** 4671–4682
31. Canova, M. J., Veyron-Churlet, R., Zanella-Cleon, I., Cohen-Gonsaud, M., Cozzone, A. J., Becchi, M., Kremer, L., and Molle, V. (2008) *Proteomics* **8,** 521–533
32. Cole, S. T., Brosch, R., Parkhill, J., Garnier, T., Churcher, C., Harris, D., Gordon, S. V., Eiglmeier, K., Gas, S., Barry, C. E., III, Tekaia, F., Badcock, K., Basham, D., Brown, D., Chillingworth, T., Connor, R., Davies, R., Devlin, K., Feltwell, T., Gentles, S., Hamlin, N., Holroyd, S., Hornsby, T., Jagels, K., Krogh, A., McLean, J., Moule, S., Murphy, L., Oliver, K., Osborne, J., Quail, M. A., Rajandream, M. A., Rogers, J., Rutter, S., Seeger, K., Skelton, J., Squares, R., Squares, S., Sulston, J. E., Taylor, K., Whitehead, S., and Barrell, B. G. (1998) *Nature* **393,** 537–544
33. Bentley, S. D., Chater, K. F., Cerdeno-Tarraga, A. M., Challis, G. L., Thomson, N. R., James, K. D., Harris, D. E., Quail, M. A., Kieser, H., Harper, D.,

Bateman, A., Brown, S., Chandra, G., Chen, C. W., Collins, M., Cronin, A., Fraser, A., Goble, A., Hidalgo, J., Hornsby, T., Howarth, S., Huang, C. H., Kieser, T., Larke, L., Murphy, L., Oliver, K., O'Neil, S., Rabbinowitsch, E., Rajandream, M. A., Rutherford, K., Rutter, S., Seeger, K., Saunders, D., Sharp, S., Squares, R., Squares, S., Taylor, K., Warren, T., Wietzorrek, A., Woodward, J., Barrell, B. G., Parkhill, J., and Hopwood, D. A. (2002) *Nature* **417,** 141–147
34. Hanks, S. K., Quinn, A. M., and Hunter, T. (1988) *Science* **241,** 42–52
35. Hanks, S. K., and Hunter, T. (1995) *FASEB J.* **9,** 576–596
36. Kyte, J., and Doolittle, R. F. (1982) *J. Mol. Biol.* **157,** 105–132
37. Yeats, C., Finn, R. D., and Bateman, A. (2002) *Trends Biochem. Sci.* **27,** 438–440
38. Boitel, B., Ortiz-Lombardia, M., Duran, R., Pompeo, F., Cole, S. T., Cervenansky, C., and Alzari, P. M. (2003) *Mol. Microbiol.* **49,** 1493–1508
39. Peirs, P., De Wit, L., Braibant, M., Huygen, K., and Content, J. (1997) *Eur. J. Biochem.* **244,** 604–612
40. Molle, V., Girard-Blanc, C., Kremer, L., Doublet, P., Cozzone, A. J., and Prost, J. F. (2003) *Biochem. Biophys. Res. Commun.* **308,** 820–825
41. Zhang, W., Inouye, M., and Inouye, S. (1996) *Mol. Microbiol.* **20,** 435–447
42. Hanlon, W. A., Inouye, M., and Inouye, S. (1997) *Mol. Microbiol.* **23,** 459–471
43. Nariya, H., and Inouye, S. (2005) *Mol. Microbiol.* **58,** 367–379
44. Shirai, T., Nakato, A., Izutani, N., Nagahisa, K., Shioya, S., Kimura, E., Kawarabayasi, Y., Yamagishi, A., Gojobori, T., and Shimizu, H. (2005) *Metab. Eng.* **7,** 59–69
45. Cowley, S., Ko, M., Pick, N., Chow, R., Downing, K. J., Gordhan, B. G., Betts, J. C., Mizrahi, V., Smith, D. A., Stokes, R. W., and Av-Gay, Y. (2004) *Mol. Microbiol.* **52,** 1691–1702
46. Koul, A., Choidas, A., Tyagi, A. K., Drlica, K., Singh, Y., and Ullrich, A. (2001) *Microbiology* **147,** 2307–2314
47. Villarino, A., Duran, R., Wehenkel, A., Fernandez, P., England, P., Brodin, P., Cole, S. T., Zimny-Arndt, U., Jungblut, P. R., Cervenansky, C., and Alzari, P. M. (2005) *J. Mol. Biol.* **350,** 953–963
48. Molle, V., Zanella-Cleon, I., Robin, J. P., Mallejac, S., Cozzone, A. J., and Becchi, M. (2006) *Proteomics* **6,** 3754–3766
49. Av-Gay, Y., and Everett, M. (2000) *Trends Microbiol.* **8,** 238–244
50. Valbuena, N., Letek, M., Ordonez, E., Ayala, J., Daniel, R. A., Gil, J. A., and Mateos, L. M. (2007) *Mol. Microbiol.* **66,** 643–657
51. Fernandez, P., Saint-Joanis, B., Barilone, N., Jackson, M., Gicquel, B., Cole, S. T., and Alzari, P. M. (2006) *J. Bacteriol.* **188,** 7778–7784
52. Ramos, A., Letek, M., Campelo, A. B., Vaquera, J., Mateos, L. M., and Gil, J. A. (2005) *Microbiology* **151,** 2563–2572
53. Sheldrick, G. M., Jones, P. G., Kennard, O., Williams, D. H., and Smith, G. A. (1978) *Nature* **271,** 223–225
54. Fadda, D., Santona, A., D'Ulisse, V., Ghelardini, P., Ennas, M. G., Whalen, M. B., and Massidda, O. (2007) *J. Bacteriol.* **189,** 1288–1298
55. Young, K. D. (2006) *Microbiol. Mol. Biol. Rev.* **70,** 660–703
56. Karczmarek, A., Martinez-Arteaga, R., Alexeeva, S., Hansen, F. G., Vicente, M., Nanninga, N., and den Blaauwen, T. (2007) *Mol. Microbiol.* **65,** 51–63
57. Kang, C. M., Nyayapathy, S., Lee, J. Y., Suh, J. W., and Husson, R. N. (2008) *Microbiology* **154,** 725–735
58. Flardh, K. (2003) *Mol. Microbiol.* **49,** 1523–1536
59. Duran, R., Villarino, A., Bellinzoni, M., Wehenkel, A., Fernandez, P., Boitel, B., Cole, S. T., Alzari, P. M., and Cervenansky, C. (2005) *Biochem. Biophys. Res. Commun.* **333,** 858–867
60. Bendt, A. K., Burkovski, A., Schaffer, S., Bott, M., Farwick, M., and Hermann, T. (2003) *Proteomics* **3,** 1637–1646
61. Wehenkel, A., Fernandez, P., Bellinzoni, M., Catherinot, V., Barilone, N., Labesse, G., Jackson, M., and Alzari, P. M. (2006) *FEBS Lett.* **580,** 3018–3022
62. Schafer, A., Kalinowski, J., Simon, R., Seep-Feldhaus, A. H., and Puhler, A. (1990) *J. Bacteriol.* **172,** 1663–1666
63. Santamaria, R. I., Gil, J. A., and Martin, J. F. (1985) *J. Bacteriol.* **162,** 463–467
64. Schafer, A., Tauch, A., Jager, W., Kalinowski, J., Thierbach, G., and Puhler, A. (1994) *Gene* (*Amst.*) **145,** 69–73
65. Jager, W., Schafer, A., Puhler, A., Labes, G., and Wohlleben, W. (1992) *J. Bacteriol.* **174,** 5462–5465